Journal of Imaging Science and Technology® 52(6): 060505–060505-8, 2008.
© Society for Imaging Science and Technology 2008

Effects of Magnet Configurations on Brush Shape in Interactive Touchdown Developing System by the Discrete Element Method

Hiroshi Mio
Kyoto Fine Particle Technology, Keihanna Interaction Plaza, Inc., Kyoto 619-0237, Japan and Research Center for Advanced Science and Technology, Doshisha University, Kyoto 610-0321, Japan
E-mail: rca04003@mail.doshisha.ac.jp

Yoshihiro Matsuoka, Junpei Kawamura, Atsuko Shimosaka, Yoshiyuki Shirakawa and Jusuke Hidaka
Department of Chemical Engineering and Materials Science, Doshisha University, Kyoto 610-0321, Japan

Kei-ichi Tanida
PT Section 2, R&D Department 52 Corporate R&D Division 2, Kyocera Mita Corporation, Osaka 540-0585, Japan

Shoichi Sakata and Takahisa Nakaue
PT Section 5, R&D Department 32 Corporate R&D Division 1, Kyocera Mita Corporation, Osaka 540-0585, Japan

Abstract. *The objective of this article is to investigate the effect of counter magnet configuration of an interactive touchdown developing system on the behavior of the brushes using the discrete element method. The shape of the magnetic brush, its shearing force acting on a development roll, or the electric potential distribution were analyzed. The magnetic brushes in the nip were crowded when the counter magnet was installed in the development roll. Their velocities also fluctuated; the brushes were pulled into the nip and returned to only a slight degree. The shearing force increases in the presence of the counter magnet because the stiffness of the magnetic brush became high, owing to the strong magnetic field. In the experimental work the toner mass adhered onto the development roll under the uninstalled condition was much larger than that with the counter magnet installed because of the reduced shearing force. The electric potential distributions around the nip also fluctuated in the presence of multiple magnetic brushes. The adhered toner mass was found to be affected by not only the shearing force but also this fluctuation of the electric field. © 2008 Society for Imaging Science and Technology.*
[DOI: 10.2352/J.ImagingSci.Technol.(2008)52:6(060505)]

INTRODUCTION

An electrophotographic system is one of the most commonly used printing technologies during the past few decades. Demand on printing technology (e.g., printing speed, high quality, low cost, energy saving, and ecological technology) are increasing with rapid development of information technologies, and new machines having innovative and unique methods are being developed in many industries every year. An interactive touchdown developing method,[1] which is shown in Figure 1, has characteristics of high print quality and high stability; i.e., it combines the advantages of both the two-component developing method and the monocomponent developing method. A two-component developer is carried by the magnet roller, and toner particles alone adhere on the surface of the development roll, forming a thin layer (two-component developing process). Then the toner particles are developed onto the latent images on the photoreceptor (monocomponent developing process). Thus, this method ensures excellent and long-lasting print quality.[1]

Although this developing method has useful characteristics, there is an important issue; i.e., that is the need to

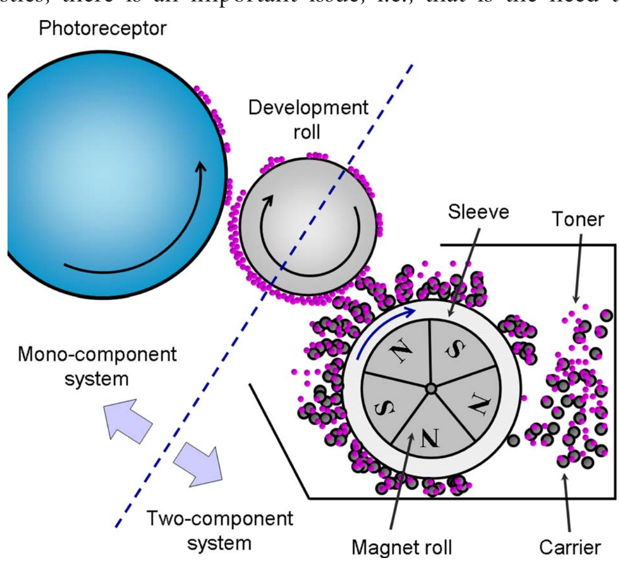

Figure 1. Schematic diagram of interactive touchdown developing method.

Received Mar. 22, 2008; accepted for publication Sep. 5, 2008; published online Dec. 10, 2008.
1062-3701/2008/52(6)/060505/8/$20.00.

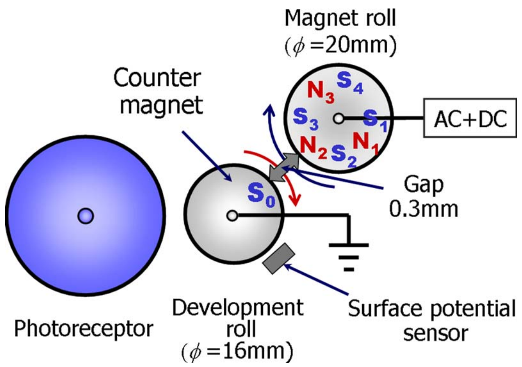

Figure 2. Schematic diagram of experimental apparatus.

reduce the imaging ghost phenomenon[2] during the monocomponent developing process. The imaging ghost is the residual image of the previous print; one of the causes of ghosting is unstable toner supply after printing (insufficient or excess). To solve this problem, quick replenishment of the consumed toner layer on the development roll is very important, and the installation of a counter magnet in the development roll at the nip of two-component developing process has been proposed to this end. It is expected that in consequence the magnetic field will be large and the magnetic brushes at the nip will have high stiffness. These changes should be effective for reducing the imaging ghost phenomenon; however, it is difficult to analyze the effects of the installation of a counter magnet on the interactive touchdown system in detail using a purely experimental approach. Thus, numerical analysis is useful to grasp the phenomena found in this system.

In this article, the behavior of the magnetic brushes in the two-component developing process was simulated using the discrete element method (DEM),[3–7] and the effects of the installation of counter magnet, its angle against the nip, and its relative coercivity on the development behavior, namely the shearing force acting on the development roll or the electric potential distribution, were evaluated.

EXPERIMENTAL

The effect of a counter magnet on the adhered toner mass on the development roll was studied in an interactive touchdown developing system, which is shown in Figure 2. This experimental apparatus was converted from a practical machine. It had a photoreceptor, however, it did not have processes for developing to the photoreceptor, transferring, or fusing. The diameters of development roll and the magnetic roll were 16 and 20 mm, respectively. The gap between them at the nip was 0.3 mm. The magnet roll consisted of seven magnets, and the counter magnet was installed in the development roll. Both rolls had sleeves, and the rotational speeds of the development roll and the magnet roll were 177.8 rpm (0.15 m/s) and 266.7 rpm (0.24 m/s), respectively, counter to each other. Figure 3 shows the magnetic flux density distribution around the nip area, which was analyzed by J-MAG, studio ver. 8.3 (JRI Solutions, Ltd.). Pulverized toner particles (d_{50}=9.1 μm) and ferritic carrier particles (d_{50}=51.3 μm) were used in this work. The toner particles were deposited onto the development roll by the magnetic brush. The surface potential on the development roll was measured using a surface potential sensor (EFS-21D, TDK Corporation), and the data were collected to a computer using a recorder (NR-110, Keyence Corporation). The distance between the surface potential analyzer and development roll was kept constant at 3.0 mm. The adhered toner mass was estimated from the surface potential. The offset bias voltage and the peak-to-peak voltage were set at 300 and 2000 V using a high voltage function generator (615-3, Trek, Inc.). The bias frequency was varied between 3.0 or 5.0 kHz. Temperature and relative humidity in the room were controlled at (22.0±1.0)°C and (38.0±4.0)%. Measurements under each condition were carried out three times and the mean values taken.

SIMULATION

The three-dimensional particle behavior in the interactive touchdown developing system was simulated using the DEM.[3] The DEM is one of the most popular and reliable simulation methods for the numerical analysis of solid particle behavior. This simulation method consists of the idea of determining the kinematic force to each finite-sized particle. All forces acting on each particle are modeled and calculated at every discrete time step. The trajectories of particles are updated by Newton's law of motion, as shown in the following equations:

$$\dot{\mathbf{v}} = \frac{\Sigma \mathbf{F}}{m_g}, \tag{1}$$

$$\dot{\boldsymbol{\omega}} = \frac{\Sigma \mathbf{M}}{I}, \tag{2}$$

where $\mathbf{v}$ is the particle velocity, $\mathbf{F}$ is the summed force acting on a particle, m_g means the mass of a particle, $\boldsymbol{\omega}$ is the angular velocity, $\mathbf{M}$ and I denote the moment of force and the moment of inertia. The contact force, $\mathbf{F}_{CT}$, magnetic force, $\mathbf{F}_M$, van der Waals force, $\mathbf{F}_v$ and gravitational force, $\mathbf{F}_G$ act on carrier particles in this system, and all forces are summed up.

Contact Force

A contact model between two particles is given by the Voigt model, which consists of a spring-dashpot and a slider for the friction in the tangential component. The contact forces, $\mathbf{F}_n$, compressive, and $\mathbf{F}_t$, shear, can be calculated by the following equations:

$$\mathbf{F}_{n,ij} = \left(K_n \Delta u_{n,ij} + \eta_n \frac{\Delta u_{n,ij}}{\Delta t} \right) \mathbf{n}_{ij}, \tag{3}$$

$$\mathbf{F}_{t,ij} = \min\left\{ \mu_f |\mathbf{F}_{n,ij}| \mathbf{t}_{ij}, \left[K_t(\Delta u_{t,ij} + \Delta\varphi_{ij}) + \eta_t\left(\frac{\Delta u_{t,ij} + \Delta\varphi_{ij}}{\Delta t}\right)\right]\mathbf{t}_{ij} \right\}, \tag{4}$$

where K and η mean the spring and the damping coefficients, which are given by Eqs. (5)–(8); Δu and $\Delta\varphi$ are a relative translational displacement of gravitational center between two particles and a relative displacement at the contact point caused by the particle rotation. The frictional coefficient is represented by μ_f (=0.58); $\mathbf{n}_{ij}$ and $\mathbf{t}_{ij}$ denote the unit vectors in normal and tangential components. The subscripts n and t indicate the normal and tangential components

$$K_n = \frac{2}{3}\cdot\frac{E}{1-\nu^2}b, \tag{5}$$

$$K_t = 8b\frac{1}{2(1+\nu)}\cdot\frac{E}{2(2-\nu)}, \tag{6}$$

$$\eta_n = 2\sqrt{mK_n}, \tag{7}$$

$$\eta_t = \eta_n\sqrt{\frac{K_t}{K_n}}, \tag{8}$$

where E and ν are Young's modulus (=0.1 GPa) and Poisson's ratio (=0.3), and b denotes the radius of the contact area.

Magnetic Force

Carrier particles in the magnetic field caused by the magnet roll form the magnetic brush on the sleeve. The magnetic force is calculated from following equations:[8]

$$\mathbf{F}_{M,i} = (\mathbf{m}_i \cdot \boldsymbol{\nabla})\mathbf{B}_i, \tag{9}$$

$$\mathbf{B}_i = \mathbf{B}_{i,\text{field}} + \sum_{j=1(\neq i)}^{n} \mathbf{B}_{i,j}, \tag{10}$$

$$\mathbf{B}_{i,j} = \frac{\mu_0}{4\pi}\left[\frac{3(\mathbf{m}_j\cdot\mathbf{R}_{ji})}{|\mathbf{R}_{ji}|^5}\mathbf{R}_{ji} - \frac{\mathbf{m}_j}{|\mathbf{R}_{ji}|^3}\right], \tag{11}$$

where $\mathbf{m}_i$ and $\mathbf{B}_{i,\text{field}}$ mean the magnetic dipole moment of ith particle and the magnetic flux density caused by the magnet roll at the position of ith particle, respectively. $\mathbf{B}_{i,j}$ is the magnetic flux density caused by the magnetized jth particle, and μ_0 is the magnetic permeability of vacuum ($=1.26\times10^{-6}$ H/m); $\mathbf{R}_{\text{ji}}$ is the position vector from jth particle to ith one. The magnetic dipole moment is defined by Eq. (12),

$$\mathbf{m}_i = \frac{4\pi}{\mu_0}\frac{\mu_r - 1}{\mu_r + 2}r_i^3\mathbf{B}_i, \tag{12}$$

where μ_r means the relative magnetic permeability ($=10^4$).

The van der Waals Force

The van der Waals force $\mathbf{F}_v$ between ith and jth particles of d_i and d_j in diameter is given by the following equation:

$$\mathbf{F}_{v,i} = -\frac{\sqrt{A_iA_j}}{12h^2}\frac{d_id_j}{d_i+d_j}\frac{\mathbf{R}_{ji}}{|\mathbf{R}_{ji}|}, \tag{13}$$

where A demotes the Hamaker constant ($=7.9\times10^{-20}$ J), and h is a surface distance between the particles. When particles are in contact, h is determined to be 0.4 nm in consideration of Born repulsion.

Electric Field Around the Nip

The toner particles, which have been carried to the nip area, fly to the development roll by the electrostatic force $\mathbf{F}_E$. A toner having q in charge receives $\mathbf{F}_E$ in the electric field $\mathbf{E}$,

$$\mathbf{F}_E = q\mathbf{E}, \tag{14}$$

$$\mathbf{E} = -\nabla\phi, \tag{15}$$

ϕ is the electric potential distribution, which is given by Eq. (16),

$$\nabla^2\phi = -\frac{\rho}{\varepsilon}, \tag{16}$$

where ρ denotes the charge density of nip area, and ε is the permittivity. The electric potential distribution in the nip is affected by being the magnetic brushes.

Simulation Conditions

The effects of the counter magnet configuration on the magnetic brushes shape were investigated. The magnetic flux density around the nip was analyzed using J-MAG Studio ver. 8.3 (JRI Solutions, Ltd.). The magnet roll had seven magnets in it, and the counter magnet was installed in the development roll, as shown in Fig. 2. The relative coercivity of counter magnet, $H_{c,S0}/H_{c,N2}$ ($S0$ and $N2$ are related to Fig. 2), was changed from 0.15 to 0.78, and its installation angle, θ_c, was also changed from −10 to +10 deg against the center of nip.

The carrier particles, 35 or 50 μm in diameter, were introduced and positioned on the sleeve; the total number of particles was 10,000. The diameters of the development roll and the magnet roll were 16 and 20 mm, respectively, and their speeds were same as in the experimental case. The axial length of the calculation area was shortened to 0.5 mm due to the calculation load, and the periodic boundary was also considered in the axial direction. The other geometric configurations are same as the experimental ones. The discrete time increment, Δt, was 1.0×10^{-8} s, and the calculation was run for 5×10^6 steps.

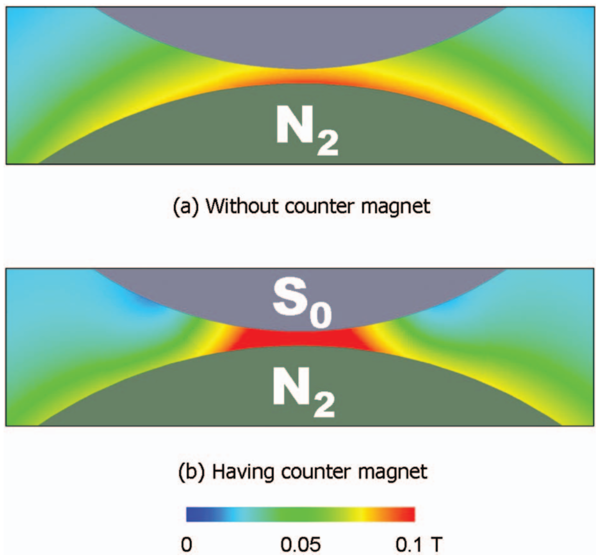

Figure 3. Magnetic flux density distribution.

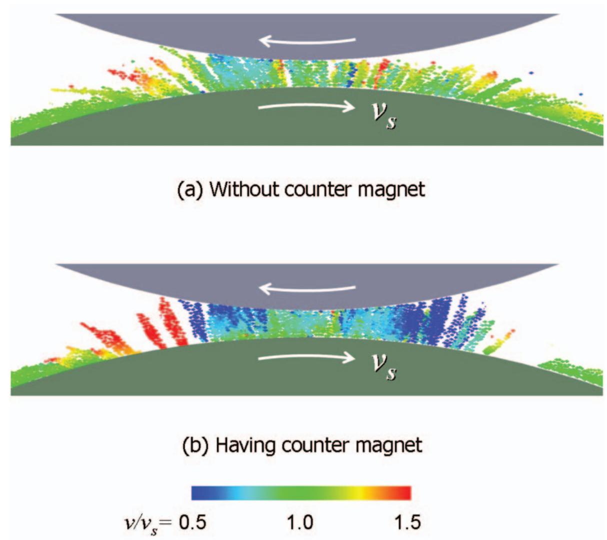

Figure 5. Snapshots of velocity of magnetic brush.

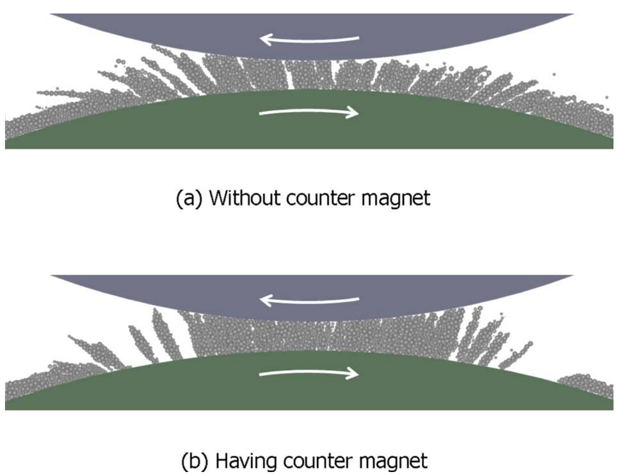

Figure 4. Snapshots of magnetic brush.

Table I. Effect of installation of counter magnet.

Counter magnet		Without	Installed
No. of carrier particles in the nip	(-)	3446.7	4741.9
Shearing force per brush contact	(μN)	1.50	3.18

The magnetic brushes around the nip affect the electric potential strongly; accordingly the effect of the permittivity of carrier particles on the calculation of electric potential distribution was considered in evaluating the effect of the brushes on the electric potential. The relative permittivity of a carrier particle was taken to be 15, and the offset bias voltage and the peak-to-peak voltage were 300 and 2000 V, respectively. The electric potential distribution was calculated using a difference method.

RESULTS AND DISCUSSIONS

Effect of the Installation of Counter Magnet on the Brush Shape

Fig. 3 shows the magnetic flux density distribution around the nip area, which was analyzed by J-MAG studio. The counter magnet having relative coercivity $H_{c,S0}/H_{c,N2}=0.45$ was installed in the development roll. It was found that the magnetic flux density distribution around the nip became extremely large when the counter magnet was installed. Figure 4 shows snapshots of the magnetic brush, as simulated by the DEM. The brush in the nip under the condition of having the counter magnet installed was crowded, and there are a few brushes just before the nip, because a strong magnetic force is acting on the carrier particles. Figure 5 shows snapshots of brush velocity. In Fig. 5 the color changes, corresponding to brush velocity changes from 0.5 v_s to 1.5 v_s, where v_s denotes the velocity of sleeve. The brush velocities are mostly the same as v_s in the absence of the counter magnet; on the other hand, they fluctuate a lot when the counter magnet is present. The velocity before the nip is accelerated to more than 1.5 v_s, and the brushes are pulled into the nip. Once the brushes come into the nip, their movements become stagnant and it is difficult for them to go out from the nip. Table I shows the mean number of carrier particles in the nip and the shearing force acting on the development roll per brush contact. The nip is defined as the area which lies ±10° from the line between the centers of magnet and development rolls. The number of carrier particles for the condition with the magnet is about 1.4 times greater than for the uninstalled condition. More toner particles when the counter magnet is present, if it is assumed that the toner particles adhere to the surface of carrier particles with same ratio. Then, new toner particles can replenish the consumed toner layer on the development roll quickly. The shearing force acting on the development roll

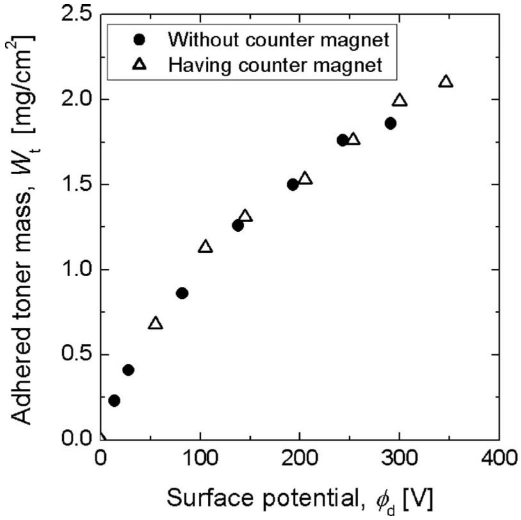

Figure 6. Relation between adhered toner mass and surface potential.

also increases when the counter magnet is present because the stiffness of the magnetic brush becomes greater due to the strong magnetic field. Thus, the consumed toner layer can be also leveled physically by shearing of the magnetic brush.

Figure 6 shows the relation between the adhered toner mass on the development roll and the surface potential in the experimental work. The relationship is independent of the magnet condition because the toner charge, which is essentially the same under both conditions, is more dominant. Thus, the adhered toner mass on the development roll can be estimated by measuring the surface potential. Figure 7 shows the change over time of adhered toner mass under 3.0 or 5.0 kHz bias frequency. The adhered toner mass increased stepwise with increasing time because more toner particles adhered with increasing number of rotations. The first step means first rotation of the development roll. It would appear that each step has a fluctuation associated with it. A lot of toner particles are transported during the first sleeve rotation because they adhere on the surface of sleeve. The rotational speed of sleeve of the magnet roll is faster than that of the development roll. Thus, a drop is seen after the first sleeve rotation. The adhered toner mass was limited due to the balance between the electrostatic force from the field and the repulsive force from the toner layer. It was found that the adhered toner mass in the absence of the counter magnet was larger than that with the counter magnet installed because of the reduced shearing force caused by the magnetic brush. The difference in adhered toner mass with and without counter magnet is very similar to of the difference in the shearing force evaluated in the simulation work. Thus, we infer that the adhered toner mass is affected by the shearing force of magnetic brush, and the simulated shear force should correlate with adhered toner mass. The time for completing the process of adhering toner to the development roll becomes short when the counter magnet is installed. Therefore, the counter magnet works well for replenishing the consumed toner layer.

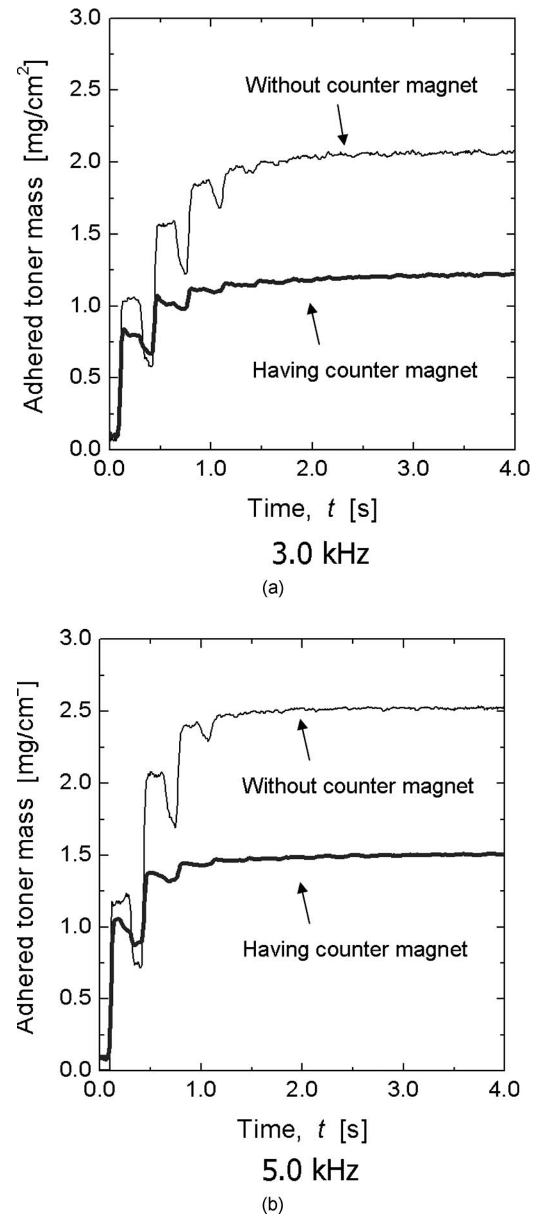

Figure 7. Time change of adhered toner mass.

Effect of the Magnet Configuration of Counter Magnet on the Brush Behavior

The behavior of the magnetic brush around the nip is affected by the magnetic field, thus to know the effect of the installation of a counter magnet seems important. Figure 8 shows the magnetic flux density distribution around the nip area under different counter magnet installation angles with $H_{c,S0}/H_{c,N2}=0.45$. The distribution corresponding to a large magnetic flux density shifted along with the position of counter magnet. Figure 9 shows snapshots of the brush velocity over the range $\theta_c=-10°$ to $+10°$. The movement of the brushes was affected by the position of counter magnet. The brush movement becomes stagnant when the counter magnet is located before the nip because the brushes stay just before the nip, and the gap length between the magnet roll and the development roll becomes small from there on so that it is difficult for the brushes to pass through the nip.

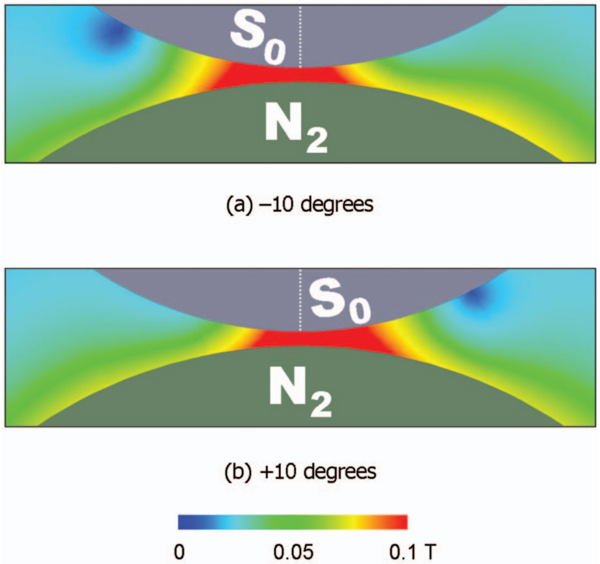

Figure 8. Magnetic flux density distribution.

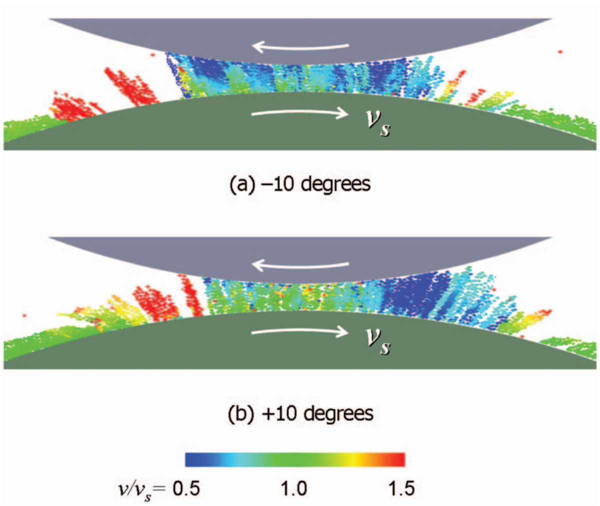

Figure 9. Snapshots of velocity of magnetic brush.

Figure 10 shows the relationship between the mean number of carrier particles in the nip and the installation angle of the counter magnet. It was found that the brush movement becomes most stagnant under the condition of ∼−5°. Figure 11 shows the relationship between the mean shearing force acting on the development roll per brush contact and the installation angle of the counter magnet. The shear force increases when the counter magnet is installed behind the nip because the magnetic brushes form against the direction of development roll rotation, which is shown in Fig. 9. Thus, the installation of the counter magnet just behind the nip will be most useful because the consumed toner layer can be replenished physically.

Figure 12 shows the magnetic flux density distribution for different counter magnet coercivities. The case where $H_{c,S0}/H_{c,N2}=0.15$ is similar to that of the uninstalled condition (Fig. 3). Figure 13 shows the snapshots of brush velocity for this condition. We found that a counter magnet having

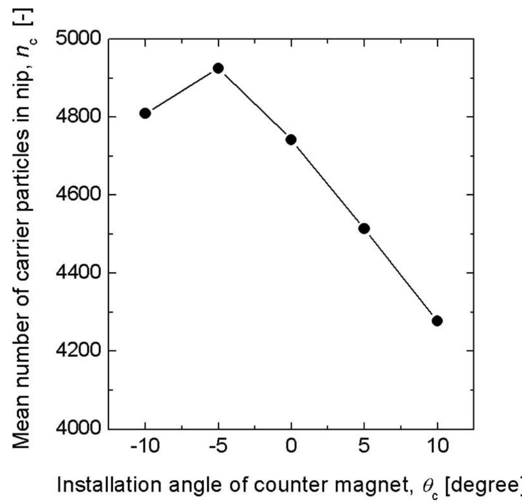

Figure 10. Relation between mean number of carrier particles in nip and installation angle of counter magnet.

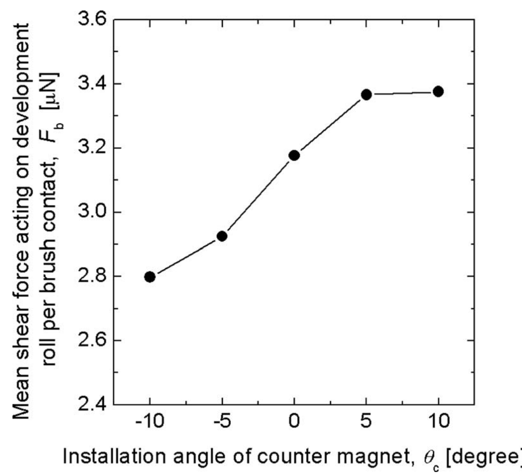

Figure 11. Relation between mean shear force acting on development roll per brush contact and installation angle of counter magnet.

small coercivity has little effect on the behavior of the brushes, and their behavior is quite similar to that without the counter magnet (Fig. 5). The nip becomes extremely crowded with many brushes, when the coercivity of the counter magnet is large. The carrier particles form connecting chains between the development roll and the magnet roll. Most brushes do not extend out from the nip due to the strong magnetic field. The shearing force acting on the development roll becomes large under this condition of large coercivity, as shown in Figure 14, and it was also found that the shearing force is directly proportional to the coercivity of counter magnet.

Figure 15 shows the equipotential surfaces around the nip having the counter magnet ($H_{c,S0}/H_{c,N2}=0.45$). It was found that the electric potential distributions fluctuated significantly. Figure 16 shows the equipotential surfaces under different magnet configurations. The fluctuation of electric potential becomes large on increasing the coercivity of the counter magnet. The adhered toner mass would be affected by not only the shearing force of the magnetic brush but also

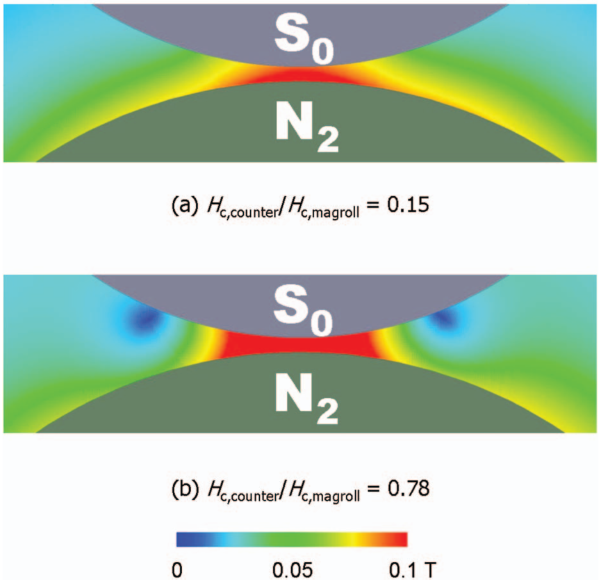

Figure 12. Magnetic flux density distribution.

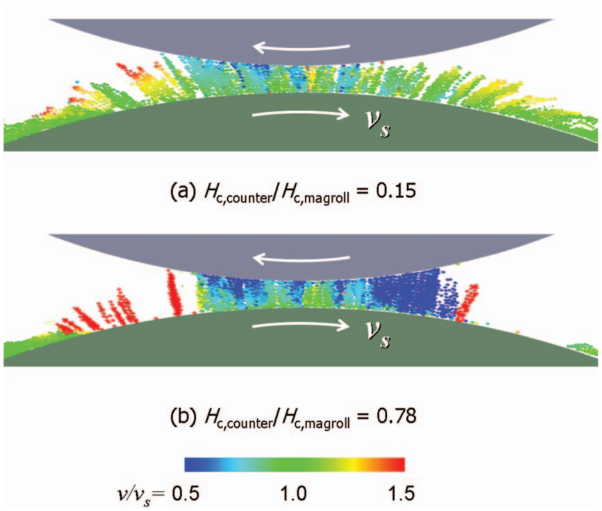

Figure 13. Snapshots of velocity of magnetic brush.

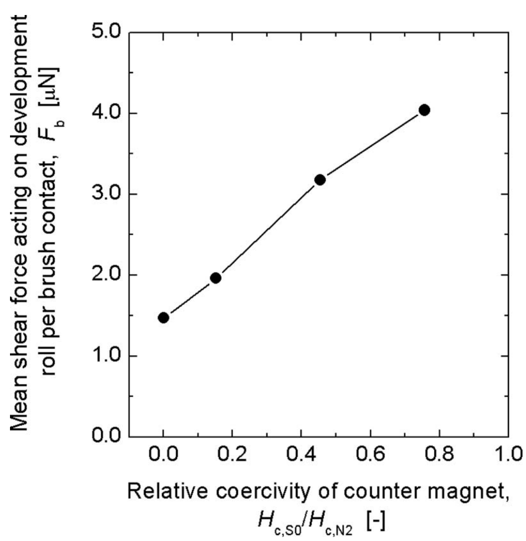

Figure 14. Relation between mean shear force acting on development roll per brush contact and relative coercivity of counter magnet.

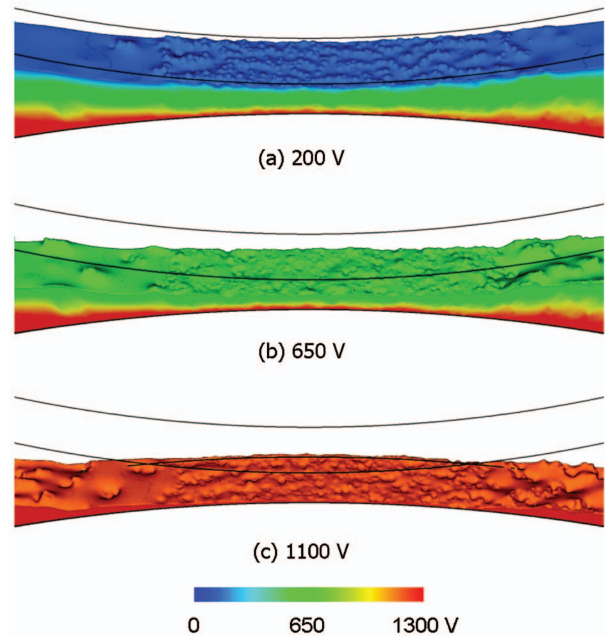

Figure 15. Snapshots of equipotential surfaces around nip having the counter magnet coercivity ratio ($H_{c,S0}/H_{c,N2}=0.45$).

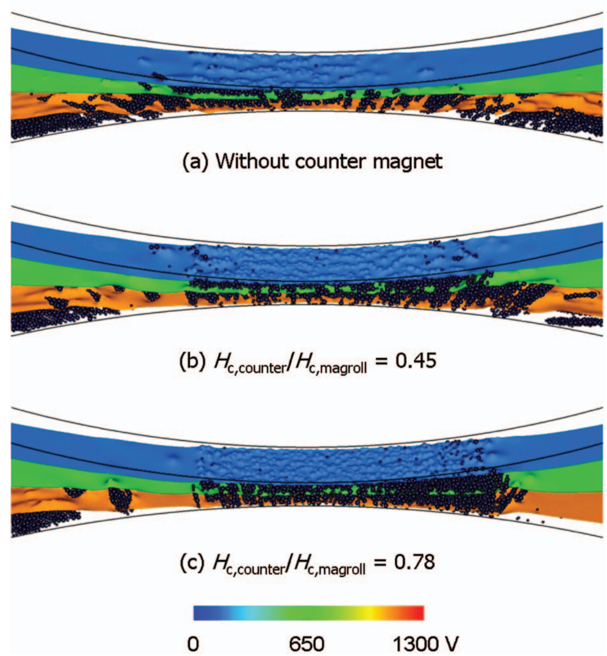

Figure 16. Snapshots of equipotential surfaces around nip.

by the condition of electric field. The effect of electric potential fluctuation on adhering toner particle behavior will be analyzed in future work by modeling two-component developers.[6]

CONCLUSIONS

The brush behavior in the interactive touchdown development system was simulated using the DEM to evaluate the effects of counter magnet configuration. A summary of the work follows.

(1) The magnetic brushes in the nip became crowed when the counter magnet was installed in the development roll. Their velocities also fluctuated; the brushes were pulled into the nip and hardly extended out of it.
(2) The shearing force acting on the development roll per brush contact increased in the presence of the counter magnet because the stiffness of magnetic brush became large due to the strong magnetic field. Thus, the consumed toner layer could be also leveled off physically by the shearing action of the magnetic brush.
(3) The adhered toner mass for the uninstalled condition in the experimental work was larger than that of installed one because of the reduced shearing force from the magnetic brush. The time for completing the deposition of toner to the development roll became short when the counter magnet was installed. Thus, the counter magnet works well for replenishing the consumed toner layer.
(4) The shearing force increased when the counter magnet was installed behind the nip because the magnetic brushes formed against the direction of development roll rotation.
(5) The counter magnet having small coercivity had little effect on the behavior of the brushes, and their behavior was quite similar to that under the uninstalled condition. The nip became extremely crowded with many brushes and most of brushes did not extend out of the nip when the coercivity was too large. It was found that the shearing force was directly proportional to the coercivity of counter magnet.
(6) The fluctuation of electric potential became large with increasing coercivity of counter magnet. The adhered toner mass is affected by not only the shearing force of magnetic brush but also the electric field.

ACKNOWLEDGMENTS

The authors are grateful to JST (Japan Science and Technology Agency) and Kyoto Prefecture Collaboration of Regional Entities for the Advancement of Technological Excellence for financial support of this project.

REFERENCES

[1] KYOCERA MITA Corporation, KYOCERA MITA GROUP Sustainability Report, 2007, p. 21.
[2] K. Aoki, H. Matsushiro, and K. Sakamoto, "The mechanism of ghost formation in a nonmagnetic single-component process", J. Imaging Sci. Technol. **40**, 359–363 (1996).
[3] P. A. Cundall and O. D. L. Strack, "A discrete numerical model for granular assemblies", Geotechnique **29**, 47–65 (1979).
[4] J. Hidaka, Y. Sasaki, A. Shimosaka, and Y. Shirakawa, "Simulation of flow behavior of tow-component developer in electro-photographic system", Adv. Powder Technol. **13**, 317–332 (2002).
[5] N. Nakayama, H. Kawamoto, and S. Yamada, "Resonance frequency and stiffness of magnetic bead chain in magnetic field", J. Imaging Sci. Technol. **47**, 408–417 (2003).
[6] H. Mio, Y. Matsuoka, A. Shimosaka, Y. Shirakawa, and J. Hidaka, "Analysis of developing behavior in two-component development system by large-scale discrete element method", J. Chem. Eng. Jpn. **39**, 1137–1144 (2006).
[7] I. E. M. Severens, A. A. F. van de Ven, D. E. Wolf, and R. M. M. Mattheji, "Discrete element method simulations of toner behavior in the development nip of the Océ Direct Imaging print process", Granular Matter **8**, 137–150 (2006).
[8] R. S. Paranjpe and H. G. Elrod, "Stability of chains of permeable spherical beads in an applied magnetic field", J. Appl. Phys. **60**, 418–422 (1986).